SASEC2015
Third Southern African Solar Energy Conference
11 – 13 May 2015
Kruger National Park, South Africa

OPTIMIZATION OF HELIOSTAT POD STRUCTURE FOR WIND LOADS

G. Delport[a], K.J. Craig[b*]
*Author for correspondence
[a]*Graduate student* [b]*PrEng, PhD, Professor*
Department of Mechanical and Aeronautical Engineering, University of Pretoria, Pretoria 0002, South Africa

ABSTRACT

There is a great need to design cost-effective heliostat arrangements for use in solar power plants. Ideal optimization of the design would be to minimize material and to allow for simple field assembly. The purpose of this study is to develop a parametric finite element model that allows for optimization of a modular heliostat structure, the HelioPod. Static wind profiles are generated using aerodynamic coefficients and steady-state ANSYS® Fluent computational fluid dynamics analyses. The heliostat base structure is built using ANSYS® finite element analysis software utilizing beam elements. These elements decrease run time and are simple enough that the geometry of the section can be easily changed. The existing frame is analyzed as base design, and 5 candidate optimum designs are determine using response surface optimization from 95 design points. In this initial study, the pylon diameter and wall thickness are shown to be the most sensitive parameters in reducing the mass and total deformation of the structure.

INTRODUCTION

Heliostat structures make up a large portion of the initial capital cost of a central receiver concentrating solar power plant (e.g., "solar towers"). As such, there is a great need to design more cost-effective heliostat arrangements. The largest contributor to the total cost of concentrating solar power is the collector field (see Figure 1 [1]).

Making heliostats modular reduces cost and assembly time. The challenge in making the structure modular and cost effective is that it still needs to be structurally stiff enough to maintain perfect focus during operation. Ideal optimization of the design would be to minimize material to allow for simple field assembly. For the solar power station, there are always hundreds of heliostats that track the sun and concentrate the sunlight into the receiver (which is fixed on the tower). Once the deformation of the heliostat structure exceeds the allowable value, the beam image will be enlarged or move out of the receiver. Wind loading is the main factor that may cause the deformation. Therefore, it is important to perform research on the wind loading and on the wind-induced dynamic performance of heliostats [2, 3, and 4].

NOMENCLATURE

C_d	[-]	drag coefficient
A	[m^3]	area
F	[N]	force
T	[K]	temperature
V	[m/s]	wind speed
x, y, z	[m]	Cartesian axis direction
rx, ry, rz	[-]]	rotational degrees of freedom
ρ	[kg/m^3]	density

Subscripts

Drag	forces acting opposite to the relative motion
X_Drag	drag forces in the x-direction
Y_Drag	drag forces in the y-direction

Abbreviations

CSP	concentrating solar power
FEA	finite element analysis
CFD	computational fluid dynamics
SST	shear stress transport
EWT	enhanced wall treatment

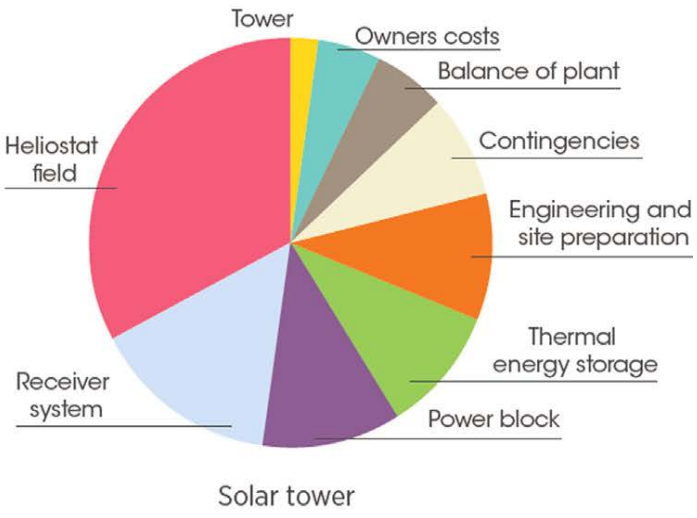

Figure 1. Current installed cost for 100MW and tower concentrating solar power plants in South Africa [1]

The purpose of this study is to develop a parametric finite element model that will allow for optimization of a modular heliostat structure, HelioPod, which is under development by Stellenbosch University's Solar Thermal Energy Research Group (STERG). The HelioPod houses six reflectors that share a common base frame and control configuration. The current base structure is not optimized.

This study will investigate different parameters that affect the layout of the base structure. Static wind loads are generated using two methods. The first method uses bluff-body aerodynamic coefficients obtained from literature. The second method uses forces and moments obtained from steady-state computational fluid dynamics (CFD) analyses at a few chosen worst-case wind directions. In this first phase, the static loads are applied to the structure in a finite element analysis (FEA) using ANSYS. Future work will include dynamic effects.

The paper first describes the FEA model and boundary conditions; where after, the methods for obtaining the wind loads (forces and moments) are outlined. This is followed by results of the base structure and then a discussion of candidate optimum designs that minimize mass and deformation, but maximum stress.

MODEL AND BOUNDARY CONDITIONS

The heliostat base structure is built using ANSYS® FEA software utilizing shell and beam elements. These elements decrease run time and are simple enough that the geometry of the section can be easily changed. The heliostat reflectors are not included in the FEA model; therefore, they are assumed to be rigid. The model was generated to simulate a typical modular heliostat structure. The geometry of the HelioPod is shown in Figure 2. The model was created in ANSYS Workbench, using higher-order beam elements. The model consists of 336 elements and 588 nodes. Beam elements were chosen to minimize the computer run time while still producing accurate results.

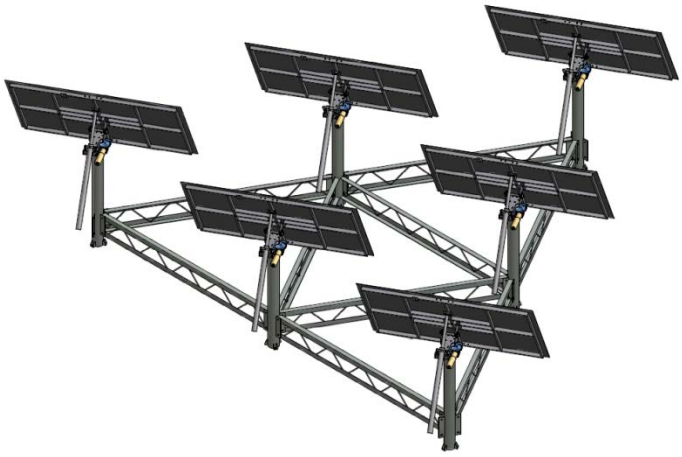

Figure 2 HelioPod geometry (heliostat reflector dimension 1.83m × 1.22m)

Figure 3 shows the FEA model with the profiles of the beam elements plotted and the numbering convention of the pylons. The beams were connected to the pylons using constraint equations. These constraint equations were set to couple the three (x, y, and z) translational degrees of freedom, but not the three (rx, ry, and rz) rotational degrees of freedom.

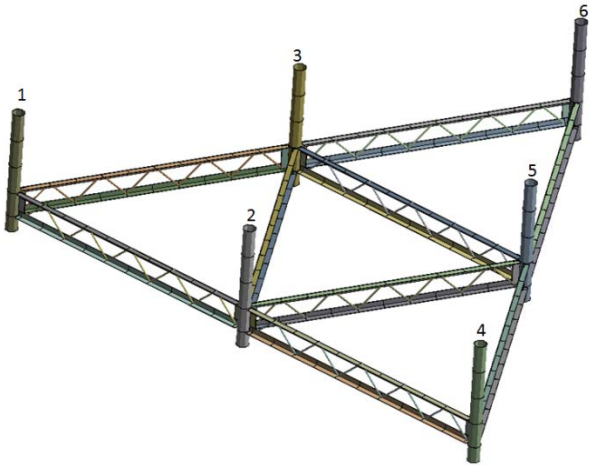

Figure 3 HelioPod support structure model

The model was constrained in all three directions of the bottom of pylon #5. The HelioPod structure can be bolted down or just set on the ground; therefore, all other pylons were constrained so that they could not translate vertically down, but could lift up. It is more conservative to not constrain the model from lifting up. A gravitational (g) force was also applied to the model. The parameters in Table 1 were chosen as variables in the optimization study described later and implemented in the ANSYS Design Modeler environment.

Table 1 Input parameters for FEA model geometry

Input Parameters			
Parameter Number	**Description**	**Start Value**	**Unit**
P1	Angle Vertical Leg	50	mm
P2	Angle Horizontal Leg	= P1	mm
P5	Bracing Round Bar Radius	4	mm
P6	Angle Vertical Leg Thickness	4	mm
P7	Angle Horizontal Leg Thickness	= P6	mm
P8	Pylon Inner Radius	55.15	mm
P9	Pylon Outer Radius	= P8 + P19	mm
P15	Lattice Girder from Ground	150	mm
P16	Lattice Girder from Top	= 921 - P15	mm
P19	Pylon Wall Thickness	2	mm

CALCULATION OF DIRECTIONAL WIND FORCE AND MOMENT

Aerodynamic coefficient calculation

A wind speed (V) of 50km/h was used to calculate a force F[N] acting on the structure. The force was calculated from [5 and 6], as shown in Equation (1).

$$F_{Drag} = C_d \left(\frac{1}{2} \rho \times V^2 \times A \right) \quad (1)$$

A drag coefficient (C_d) of 2 was chosen for an infinitely large rectangular flat plate [5].

There are many possible directions from which wind can impose loads on this structure. These wind loads are applied to the structure as static loads at the attachment points of the six reflectors. To limit the amount of load cases and to narrow down the most limiting wind direction, wind loads were applied in 10° increments. The vector component of the drag force was calculated using Equations (2) and (3). The calculated force components from the FEA are shown in Table 2.

$$F_{x\_drag} = F_{Drag} \times \cos\left(\theta \times \frac{\pi}{180}\right) \quad (2)$$

$$F_{y\_drag} = F_{Drag} \times \sin\left(\theta \times \frac{\pi}{180}\right) \quad (3)$$

The maximum stress was calculated using an ANSYS FEA to be 10° relative to the x-axis. The deformation is tabulated for all wind directions considered in Table 2. The maximum deflection is also shown, and the deformation of the frame at the worst condition is displayed in Figure 4.

Table 2 HelioPod coefficient wind loads for different wind directions

Wind Angle (°)	Xcomp (N)	Ycomp (N)	Max Deflection (mm)
0	527.5723	0	0.13741
10	519.5573	-91.612	**0.13857**
20	495.7558	-180.44	0.13828
30	456.891	-263.786	0.13674
40	404.1439	-339.117	0.13453
50	339.117	-404.144	0.13454
60	263.7862	-456.891	0.13331
70	180.4404	-495.756	0.13076
80	91.61198	-519.557	0.12693
90	3.23E-14	-527.572	0.12318
100	-91.612	-519.557	0.12549
110	-180.44	-495.756	0.12945
120	-263.786	-456.891	0.13217
130	-339.117	-404.144	0.1336
140	-404.144	-339.117	0.13426
150	-456.891	-263.786	0.13663
160	-495.756	-180.44	0.13803
170	-519.557	-91.612	0.13816
180	-527.572	-6.5E-14	0.13683

CFD calculation of wind force

From a practical standpoint, it is not possible to obtain the same load on all the heliostat mirrors due to the staggered spacing that is used. An ANSYS Fluent Version 15.0 CFD model was built to calculate the various forces and moments on each of the heliostat mirrors. Two models were made; the difference between the models was the wind direction (as shown in Figure 5). The two models have opposite wind directions, both of which are expected to represent worst cases due to the upright heliostat elevation that was considered. The CFD used a different axis system than the FEA. The 0° wind force (Figure 5a) produced the largest forces on the structure; therefore, it was chosen as the limiting case for optimization to follow.

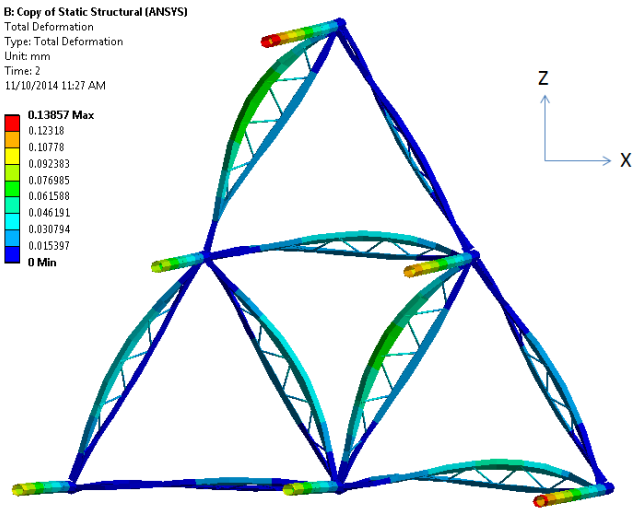

Figure 4 HelioPod maximum deformation (10° worst-case wind angle) for forces calculated using aerodynamic coefficients

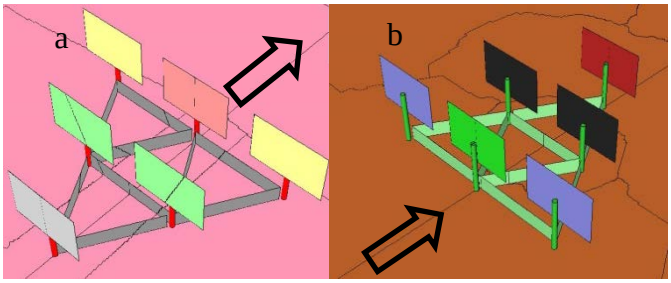

Figure 5 Two HelioPOD wind orientations considered in CFD model a) 0°, b) 180°

The heliostat design requirements [1 and 7] specify that the heliostat should be able to withstand a 50 mph (80 km/h) wind in any direction; therefore, a 50 mph (80 km/h) wind was applied in the CFD as a uniform inlet profile, again representing a worst case rather than considering an atmospheric boundary layer [8]. Forces and moments on the heliostat mirrors were calculated on the front and back from the pressures, as shown in Figures 6 and 7.

The CFD model is solved for fully turbulent flow. Both the realizable k-ε turbulence model, with enhanced wall treatment, and the SST k-ω turbulence model were evaluated on a computational mesh numbering approximately 15.3 million cells. The symmetrical computational domain extended to a half-width of 26.2 m, a height of 20.9 m, an upstream length of 15.7 m, and a downstream length of 40 m.

Table 3 shows that the SST k-ω turbulence model provides slightly larger forces than the realizable k-ε model for the 0° wind direction. Table 4 gives the moments on each heliostat for the 0° wind direction for the SST k-ω turbulence model. The symmetry of the model reflects the values.

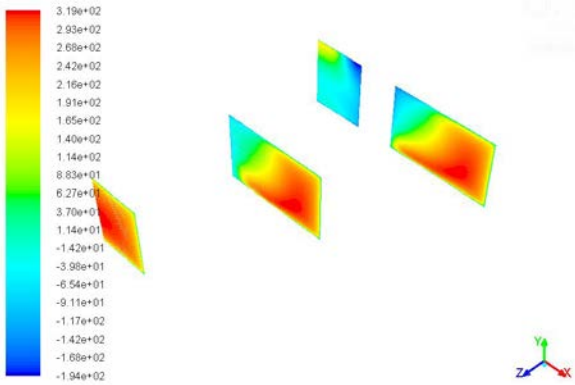

Figure 6 Pressure contours on front faces (0° direction)

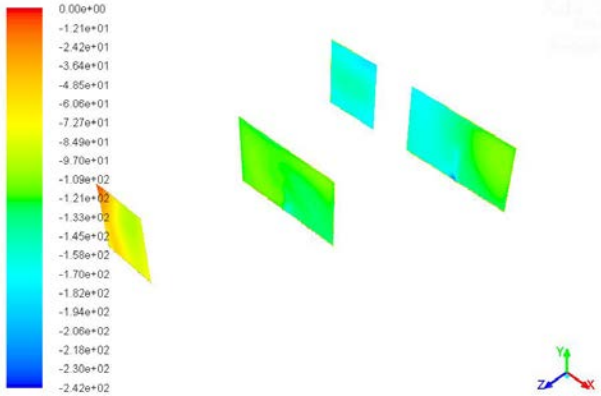

Figure 7 Pressure load on rear faces (0° direction)

Table 3 Calculated drag forces on heliostats in HelioPod (0° direction)

Heliostat		Turbulence model	
Number	Face	SST k-ω	Realizable k-ε EWT
#		Force in Z-direction	
		[N]	[N]
1	Front	-572.693	-572.494
1	Back	-165.15	-138.594
1	**Total**	**-737.842**	**-711.088**
2	Front	-393.426	-397.911
2	Back	-271.828	-219.105
2	**Total**	**-665.254**	**-617.015**
3	Front	-393.426	-397.911
3	Back	-271.828	-219.105
3	**Total**	**-665.254**	**-617.015**
4	Front	-387.64	-373.372
4	Back	-315.015	-248.945
4	**Total**	**-702.656**	**-622.316**
5	Front	70.3681	32.66298
5	Back	-360.335	-313.292
5	**Total**	**-289.967**	**-280.629**
6	Front	-387.64	-373.372
6	Back	-315.015	-248.945
6	**Total**	**-702.656**	**-622.316**

Table 4 Calculated moments on heliostats in HelioPod (0° direction) – CFD coordinate system

Heliostat Number	Moment about x-axis	Moment about Y-axis	Moment about Z-axis
	[Nm]	[Nm]	[Nm]
1	10.064	0	0
2	35.731	-140.92	0
3	35.731	140.921	0
4	46.570	-117.85	0
5	-19.134	0	0
6	46.570	117.85	0

FEA OPTIMIZATION MODEL

The forces (Table 3) and moments (Table 4) from the CFD model were applied to the beam model (as shown in Figure 8) to simulate the worst wind loading that the HelioPod in isolation can experience under normal operation. The resulting maximum combined stress (MPa) and total deformation (mm) on the structure are displayed in Figures 9 and 10, respectively. The stresses are far below any failure limits, implying that the deformation, especially as linked to the tracking accuracy of the heliostats attached to the pylons, would be the deciding performance parameter in an optimization study.

The output parameters for the baseline case were calculated in the model (Table 5) to judge the performance of the optimum design.

Each variable was assigned maximum and minimum values to bound the design. An experimental design was constructed in ANSYS DesignXplorer containing 95 points. Figure 11 shows the sensitivities of the output parameters to the various input parameters (defined in Table 1). It is shown that the most dominant parameters are parameter P8 (Pylon inner radius) and P19 (Pylon wall thickness). This is an indication that a thicker pylon will decrease the total deformation of the structure. The angle of the girder plays a smaller roll due to a twisting motion of the girder.

A design optimization analysis was done in ANSYS DesignXplorer to determine to five candidate optimum design points. The optimization was set to minimize the mass and stress. It was tasked to find the parameter set that would yield a zero deformation. Table 6 lists the result of the five optimized candidate points. It is shown that candidate point 4 is the most favourable point because it has the smallest mass and second smallest deflection. Although candidate point 5 had the smallest deflection, the mass was the largest, making this a more expensive design. The maximum combined stress and total deformation for candidate point 4 are depicted in Figures 12 and 13, respectively.

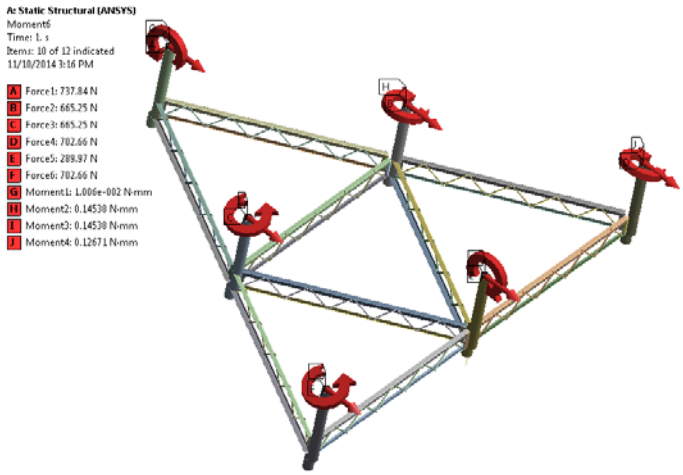

Figure 8 HelioPod wind forces and moments as applied to FEA model

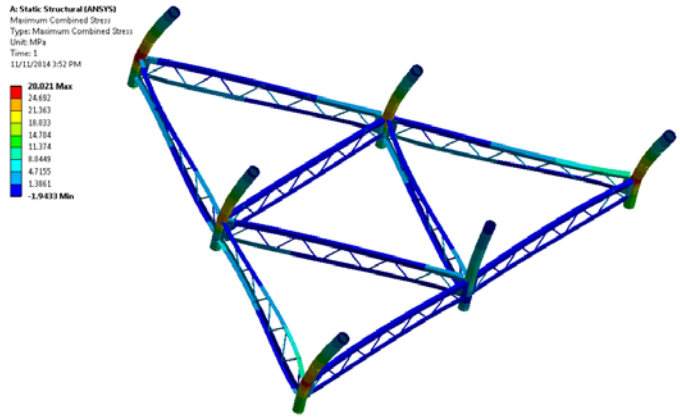

Figure 9 Baseline model maximum combined stress (MPa)

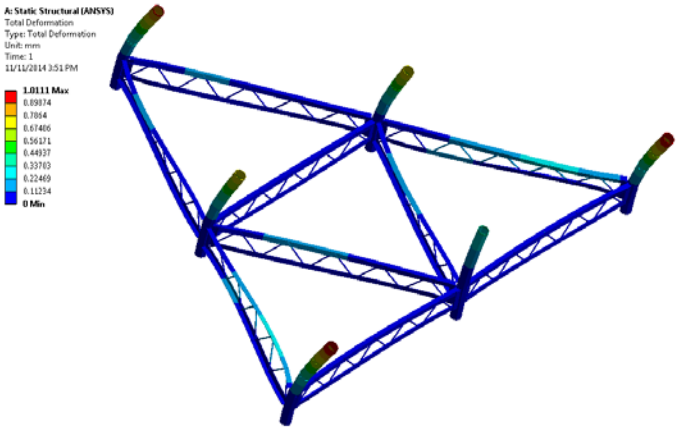

Figure 10 Baseline model total deformation (mm)

Table 5 Baseline output parameters used for optimization study

Output Parameters			
P11	Mass	0.2288	tonne
P17	Maximum Total Deformation	1.0111	mm
P18	Maximum Combined Stress	28.21	MPa
P20	Direct Stress Maximum	5.989	MPa

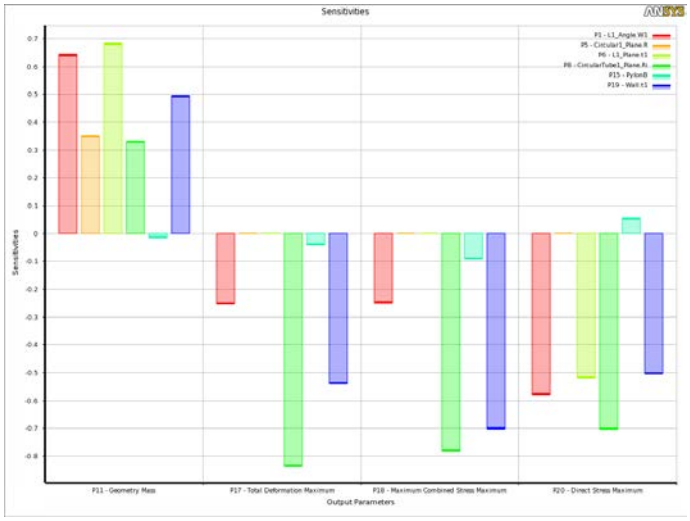

Figure 11 Output parameter sensitivities

Table 6 Optimal Design Candidates

		Candidate Point				
Parameter	**Unit**	**1**	**2**	**3**	**4**	**5**
P1	(mm)	39.80	31.80	49.40	37.40	63.80
P5	(mm)	3.69	3.91	3.36	5.00	4.18
P6	(mm)	3.21	3.80	2.81	2.32	2.48
P8	(mm)	88.25	80.25	78.65	76.25	83.45
P15	(mm)	219.17	232.23	297.53	238.76	157.59
P19	(mm)	1.61	2.11	2.21	2.95	3.10
P11	(tonne)	0.1563	0.1611	0.1740	0.1681	0.2219
P17	(mm)	0.40	0.41	0.40	0.34	0.28
P18	(MPa)	13.17	11.80	10.82	9.62	8.56
P20	(MPa)	4.55	5.04	4.59	5.37	2.31

A trade-off chart is shown in Figure 14. The blue markers show the most feasible design. There is a gradual transition to red markers, which show the worst design. Out of the possible 95 design points, ±25 points seem feasible for this design. The response surface shown in Figure 15 allows for a graphic view of the impact that parameters have on one another. In this case, the total deformation (P17) is plotted versus the pylon parameters of the inner radius (P8) and the pylon wall thickness (P19). A very large diameter pylon with a large wall thickness will minimize deflection (lowest point on response surface), but it would be heavy and costly. A constraint on the optical tracking and aiming accuracy of the heliostats (to be considered in future work) would prescribe an allowable deformation (both translational and rotational), thereby selecting the optimal combination of these parameters.

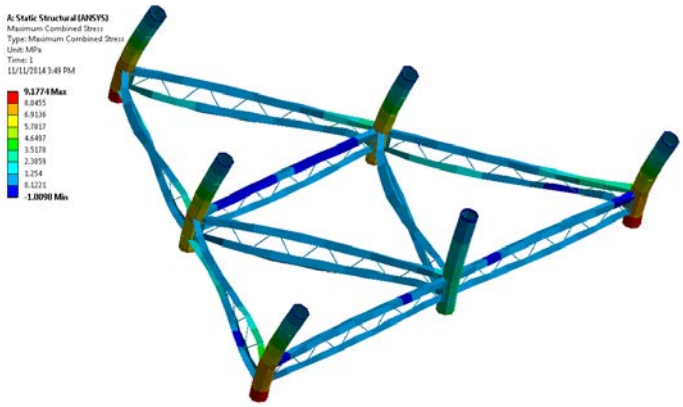

Figure 12 Candidate point 4 maximum combined stress (MPa)

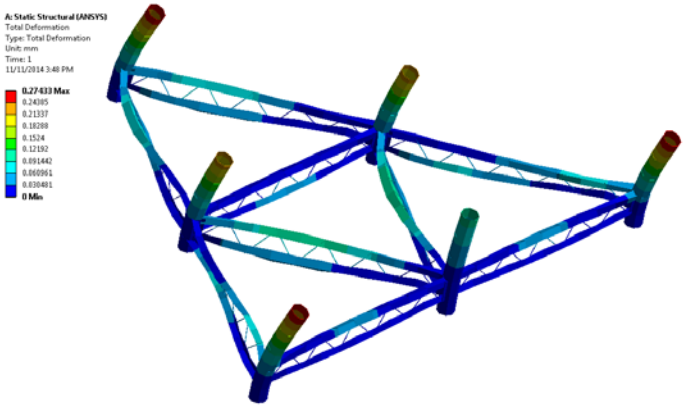

Figure 13 Candidate point 4 total deformation (mm)

CONCLUSION

An FEA analysis of the HelioPod with wind loads in the forms of forces and moments (as obtained from a CFD analysis) was performed for a static worst-case scenario. The analysis showed that the support frame structure of the HelioPod can be optimized by changing some of the key geometrical parameters using ANSYS Workbench. Based on a set of optimum candidate points, the mass of the structure can be reduced by 27%, with a decrease in the maximum deflection from 1.01 mm to 0.34 mm. By reducing the mass, the material cost of the structure will be lower. Further investigation can be done to reduce the manufacturing costs of welding and ease the assembly process.

ACKNOWLEDGEMENTS

The authors would like to acknowledge the support from the University of Pretoria (South Africa), the South African National Research Foundation (DST-NRF Solar Spoke), as well information provided by the Solar Thermal Energy Research Group (STERG) at Stellenbosch University (South Africa).

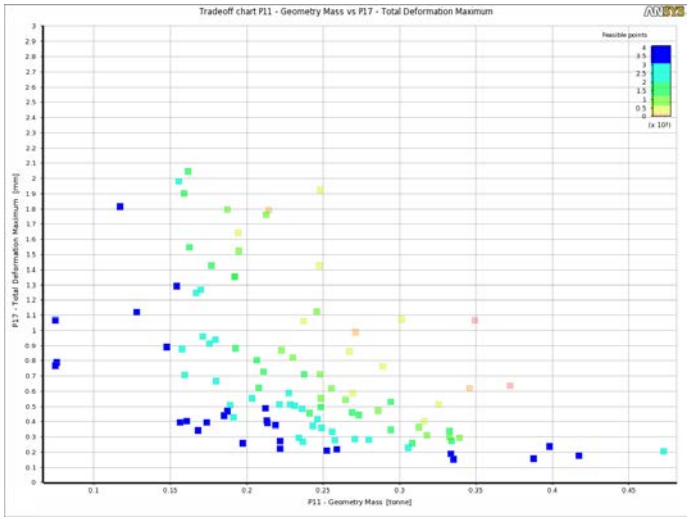

Figure 14 Trade-off chart – Mass (P19) (tonne) versus Total Deformation (P17) (mm)

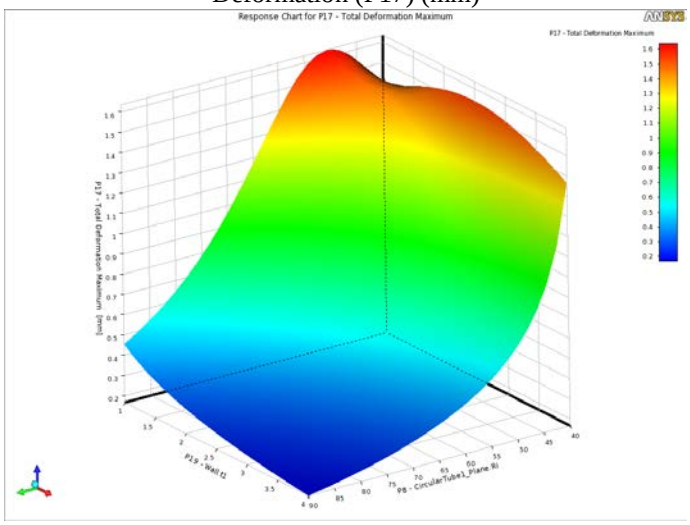

Figure 15 Response surface for P17 Total Deformation (mm) as a function of P19 (Pylon wall thickness) and P8 (Pylon inner radius)

REFERENCES

[1] Honghang Sun , Bo Gong, Qiang Yao.*A review of wind loads on heliostats and trough collectors* Renewable and Sustainable Energy Reviews 32 (2014) 206–221

[2] C.C. Zanga, J. M. Christian, J. K. Yuan, J. Sment, A. C. Moya, C. K. Ho, and Z.F.Wang *Numerical simulation of wind loads and wind induced dynamic response of heliostats* Energy Procedia 49 (2014) 1582 – 1591

[3] Badhuri, S. and Murphy, L.M.,*Wind Loading on Solar Collectors*, Solar Energy Research Report, TR-253-2169, 1985.

[4] Bo Gong, Zhengnong Li, Zhifeng Wang, Yingge Wang *Wind-induced dynamic response of Heliostat* Renewable Energy 38 (2012) 206-213

[5] White, Frank M. *Fluid mechanics* 7th ed., 2011.

[6] Strachan JW. *Testing and evaluation of large-area heliostats for solar thermal applications.* Technical Report for Sandia Laboratories. Report No. SAND92- 1381; 1993.

[7] Mavis CL. *A description and assessment of heliostat technology*. Technical Report for Sandia Laboratories. Report No. SAND87-8025; 1987.

[8] Hachicha, A.A., *Numerical modelling of a parabolic trough solar collector*, PhD Thesis, 2013, Universitat Politècnica de Catalunya.